Available online at www.sciencedirect.com
SCIENCE DIRECT®
Thermochimica Acta 405 (2003) 279–285
thermochimica acta
www.elsevier.com/locate/tca

The effect of substitution on the thermo-physical properties of $LaMn_xV_{1-x}O_{4-\delta}$

S. Varma, B.R. Ambekar, B.N. Wani, N.M. Gupta*

Applied Chemistry Division, Bhabha Atomic Research Centre, Trombay, Mumbai-400 085, India

Received 19 September 2002; received in revised form 10 January 2003; accepted 31 March 2003

Abstract

$LaMn_xV_{1-x}O_{4-\delta}(0 \leq x \leq 1)$ samples were characterized using thermogravimetry, thermo-dilatometry, high-temperature X-ray diffraction (HTXRD) and temperature-programmed reduction techniques, with an objective to explore the role of substitution on their thermo-physical properties, which may have a direct bearing on their catalytic behavior. Even though the substituted compositions ($x < 0.8$) were of a single phase, their reduction occurred in two steps, a lower temperature step corresponding to $Mn^{4+} \rightarrow Mn^{3+}/Mn^{2+}$ and another higher temperature one related to $V^{5+} \rightarrow V^{3+}$. The dilatometric measurements gave similar values of linear thermal expansion coefficient (α_1) at temperatures up to 600 °C, both for $LaVO_4$ and substituted samples. A different behavior was, however, observed at higher temperatures, whereas thermal contraction was observed in case of $LaVO_4$ for measurements at temperatures above 700 °C, the value of α_1 remained almost constant in case of the substituted samples. Furthermore, the HTXRD data revealed expansion in cell volume for all temperatures up to 950 °C, irrespective of the substitution. These results therefore point to a higher degree of sintering in $LaVO_4$ as compared to Mn-doped samples on heating at temperatures above 700 °C. It is inferred that the resistance to sintering and the lowering of the reduction temperature are both responsible to the higher catalytic activity of the substituted samples and their compositional stability during the repeated cycles of reduction–reoxidation, as reported earlier [Appl. Catal. A 205 (2001) 295].

Keywords: Orthovanadate; TG; TPR; HTXRD; Dilatometry; Role of substitution

1. Introduction

Mixed oxides with spinel, perovskite and pyrochlore structures have been investigated widely in order to explore their suitability as catalysts for various applications such as in pollution control, electrolytic cells, etc. Among these oxide systems, the simple perovskites with basic formula ABO_3 have received much of the attention [1–4]. A main hindrance in acceptance of such catalysts has been their instability under long-term reaction conditions. We have taken up in our laboratory a systematic study on the catalytic behavior of oxygen-rich ABO_4-type compounds in order to demonstrate the influence of substitution at A or B site on the catalytic activity and the compositional stability of these compounds during the repeated cycles of oxidation and reduction. In a recent publication, we reported that even though the lanthanum orthovanadate ($LaVO_4$) showed a very limited activity for CO oxidation reaction, the substitution of V^{5+} by Mn^{4+} led to a remarkable improve-

* Corresponding author. Fax: +91-22-550-5151.
E-mail address: nmgupta@magnum.barc.ernet.in (N.M. Gupta).

0040-6031/$ – see front matter © 2003 Elsevier B.V. All rights reserved.
doi:10.1016/S0040-6031(03)00199-0

ment in catalytic activity and it also resulted in greater structural stability over repetitive cycles of reduction and re-oxidation [5]. The oxygen non-stoichiometry generated in the system on introduction of Mn^{4+} is found to be responsible for this improvement. Present study was taken up to monitor the thermo-physical characteristics of $LaMn_xV_{1-x}O_{4-\delta}$ compositions using thermogravimetry (TG), temperature-programmed reduction (TPR), thermo-dilatometry and high-temperature X-ray diffraction (HTXRD) techniques, with a view to understand the role of substitutions in the modification of the structural and catalytic properties of these compounds.

2. Experimental

$LaMn_xV_{1-x}O_{4-\delta}$ ($0 \leq x \leq 1.0$) samples were prepared by ceramic route, as described earlier [5]. The samples were found to be stable when heated in air at temperatures up to 1000 °C. X-ray diffraction (XRD) patterns of different samples were recorded prior to and after TG scan on a Philips PW1710 diffractometer (Ni-filtered Cu Kα radiation). HTXRD patterns were recorded in air at scanning rate of $1^\circ\,min^{-1}$ and at temperature intervals of 200 °C with the help of a Philip X'pert Pro unit equipped with an Anton Par high-temperature attachment. The program used for generating lattice parameter from powder XRD pattern was POWD program, version 2.2 [6]. TG scans were recorded on TG-DT 30 Shimadzu thermobalance in H_2 atmosphere (8% in Ar) with sample size of few milligrams and at a heating rate of $6\,^\circ C\,min^{-1}$. The amount of H_2 consumed was calculated independently from TPR data obtained with a Thermoquest TPDRO-1100 analyzer. The TPR patterns were recorded in a temperature interval of 27–900 °C (heating rate: $6\,^\circ C\,min^{-1}$; gas flow: $20\,ml\,min^{-1}$) in the atmosphere of H_2 (5%) + Ar. The bulk thermal expansion of these mixed oxide samples was monitored in air in the range of ambient temperature to 900 °C, using an LKB 3185 fused quartz vertical thermo-dilatometer. For these measurements the samples were pelletized (10 mm diameter) at the same pressure of $4000\,kg\,cm^{-2}$. The bulk density of the two typical sample pellets of $LaVO_4$ and $LaMn_{0.5}V_{0.5}O_{4-\delta}$ thus prepared was found to be 3.56 and $2.75\,g\,cm^{-3}$, respectively.

3. Results and discussion

3.1. X-ray diffraction

All the compositions of $LaMn_xV_{1-x}O_{4-\delta}$ samples ($x = 0.0$–0.8) were found to be of single phase and their XRD powder patterns matched with the typical XRD diffraction of monoclinic $LaVO_4$ (JCPDS card no. 25-427). These data are described in detail in our earlier publication [5]. A slight increase in peak width, however, indicated a marginal decrease of crystallinity as a result of substitution of Mn in place of V. Also, the structure of the sample with $x = 1$ was found to be different from that of both $LaVO_4$ and $LaMnO_3$, and based on the stoichiometric ratio of La_2O_3 and MnO_2 (1:2) it was deduced to be $A_2B_2O_7$-type mixed oxide.

3.2. Thermogravimetry

Fig. 1 shows the TG curves of various $LaMn_xV_{1-x}O_{4-\delta}$ compositions recorded in hydrogen atmosphere.

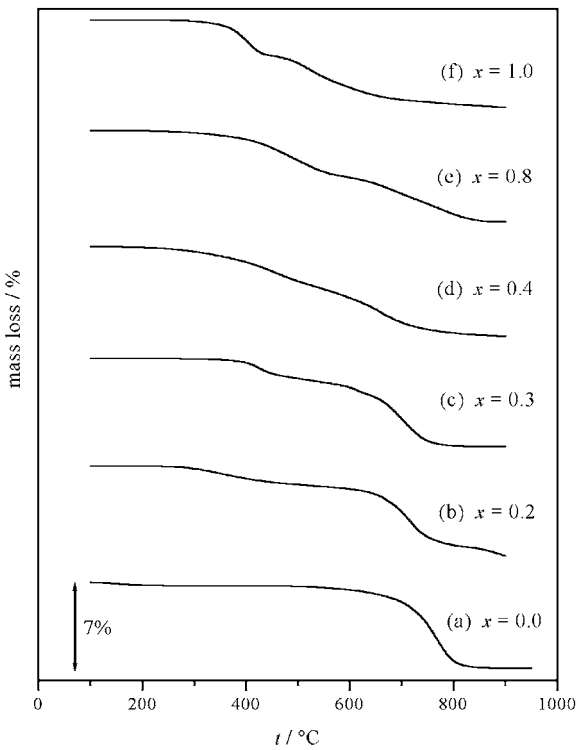

Fig. 1. TG curves of $LaMn_xV_{1-x}O_{4-\delta}$ compositions with the varying values of x.

Table 1
Thermogravimetric analysis of $LaMn_xV_{1-x}O_{4-\delta}$ in 8% H_2 in argon atmosphere

Composition	First step		Second step		Residue
	Weight loss (%)	Temperature range (°C)	Weight loss (%)	Temperature range (°C)	
V_2O_5	–	–	17.66	525–840	V_2O_3
$LaVO_4$	–	–	6.57	510–790	$LaVO_3$
$LaMn_{0.2}V_{0.8}O_{3.9}$	2.0	300–380	7.0	510–740	$LaMn_{0.2}V_{0.8}O_3$
$LaMn_{0.3}V_{0.7}O_{3.85}$	2.0	340–420	5.0	500–745	$LaMn_{0.3}V_{0.7}O_3$
$LaMn_{0.4}V_{0.6}O_{3.8}$	3.0	300–550	3.3	570–710	$LaMn_{0.4}V_{0.6}O_3$
$LaMn_{0.8}V_{0.2}O_{3.6}$	4.8	320–500	5.2	560–820	$LaVO_3$, La_2O_3, MnO
$La_2Mn_2O_7$	3.0	310–420	3.7	430–810	La_2O_3, MnO
MnO_2	22	80–690	–	–	MnO

As is evident from Fig. 1a, $LaVO_4$ shows a single step reduction in 500–800 °C temperature range. Compared to this, the Mn-substituted samples exhibited different weight loss behaviour depending upon the value of x. Thus, in case of samples with x up to 0.3 a two-step weight loss is observed (Fig. 1b–e) where the first reduction occurs in temperature region of 300–500 °C and the second reduction in 550–800 °C range. On the other hand, a multi step reduction process is observed for the samples with $x > 0.3$. In the substituted oxides there are two reducible cations, viz. manganese and vanadium. Therefore, the TG curves of these mixed oxides were evaluated in reference to pure V_2O_5 and MnO_2. On comparing the weight loss and the temperature interval during which the weight loss occurs (Table 1), one can conclude that at lower concentration of Mn in $LaMn_xV_{1-x}O_{4-\delta}$ samples ($x \leq 0.3$), Mn^{4+} reduces to Mn^{3+} in the first stage, while the second stage corresponds to the reduction of V^{5+} to V^{3+}. On the other hand, in case of samples with higher concentration of Mn ($x \geq 0.4$), while Mn^{4+} reduces to Mn^{3+} in the first step, in the second step Mn^{3+} reduces further to Mn^{2+} along with the reduction of V^{5+} to V^{3+}. This explains the multi-step TG curves in Fig. 1c–e. The XRD patterns of the residual samples obtained after the TG analysis of sample compositions with $0.5 \leq x \leq 0.8$ matched with that of $LaVO_3$, and only traces of La_2O_3 and MnO could be detected. Even though the formation of MnO remained undetected in the XRD pattern of $LaMn_{0.4}V_{0.6}O_{4-\delta}$ (Table 1) recorded after reduction, the TG data revealed that a part of Mn^{3+} is further reduced to Mn^{2+} in this sample also. TG results of Fig. 1e reveal a two-step reduction for $LaMn_{0.8}V_{0.2}O_{4-\delta}$ where a considerable weight loss is observed during the second step. The XRD pattern of the TG residue of this sample showed presence of MnO, suggesting that further reduction of Mn^{3+} to Mn^{2+} contributed to the second step along with the reduction of V^{5+} to V^{3+}. This inference is supported further by the observation that vanadium-free $LaMn_2O_7$ also showed a thermal decomposition in the temperature interval of 310–810 °C.

Thus, the overall reduction processes of $LaMn_xV_{1-x}O_{4-\delta}$, as deduced from TG data and from the XRD data recorded on residues of TG runs, can be represented by the following three possible routes depending upon sample composition:

(i) For $0.0 \leq x \leq 0.3$

$$LaMn_x{}^{4+}V_{1-x}{}^{5+}O_{4-\delta} \rightarrow LaMn_x{}^{3+}V_{1-x}{}^{5+}O_{4-\delta-x/2}$$

$$LaMn_x{}^{3+}V_{1-x}{}^{5+}O_{4-\delta-x/2} \rightarrow LaMn_x{}^{3+}V_{1-x}{}^{3+}O_3$$

(ii) For $0.4 \leq x \leq 0.8$

$$2LaMn_x{}^{4+}V_{1-x}{}^{5+}O_{4-\delta} \rightarrow 2yLaMn_x{}^{3+}V_{1-x}{}^{5+}O_{4-\delta} + (1-y)La_2O_3 + (1-y)Mn_2O_3$$

$$2yLaMn_x{}^{3+}V_{1-x}{}^{5+}O_{4-\delta} + (1-y)La_2O_3 + (1-y)Mn_2O_3 \rightarrow LaMn_x{}^{3+}V_{1-x}{}^{3+}O_3 + La_2O_3 + MnO$$

(iii) For $x = 1.0$

$$La_2Mn_2O_7 \rightarrow La_2O_3 + Mn_2O_3$$

$$La_2O_3 + Mn_2O_3 \rightarrow La_2O_3 + 2MnO$$

3.3. TPR studies

Fig. 2 presents TPR profiles of $LaMn_xV_{1-x}O_{4-\delta}$ samples. The derivative thermogravimetry (DTG) curves corresponding to the data given in Fig. 1 are also presented by dashed lines in Fig. 2 for a comparative evaluation. As seen in Fig. 2a, the first cycle of TPR profile of $LaVO_4$ comprises of a main peak with a temperature maximum (T_{max}) of ~800 °C along with a weak band at around ~600 °C. The doping with manganese led to significant changes in TPR profile. Thus, the manganese-containing samples gave rise to a multi-step reduction profile and at the same time the T_{max} of the main TPR peak (820 °C) shifted progressively to a lower temperature of 620 °C with increasing x. The data in Fig. 2 also reveal that the TPR profiles are quite in agreement with the derivative thermogravimetric plots. Since the TG data show that the reduction of Mn precedes that of vanadium in a substituted sample, the new TPR band at ~400 °C in Fig. 2b–f may be attributed to the reduction of manganese while the 800 °C peak arises due to reduction of vanadium. The progressive lowering of the temperature of the 800 °C peak in Fig. 2a–e thus indicates an ease of reduction of vanadium as a result of Mn doping. The XRD profile of the residue obtained after TPR runs matched with that of $LaVO_3$ (JCPDS card no. 11–24). The hydrogen consumption data for TPR runs indicate a consistent increase in the value of δ (oxygen ion vacancies) with increasing value of x.

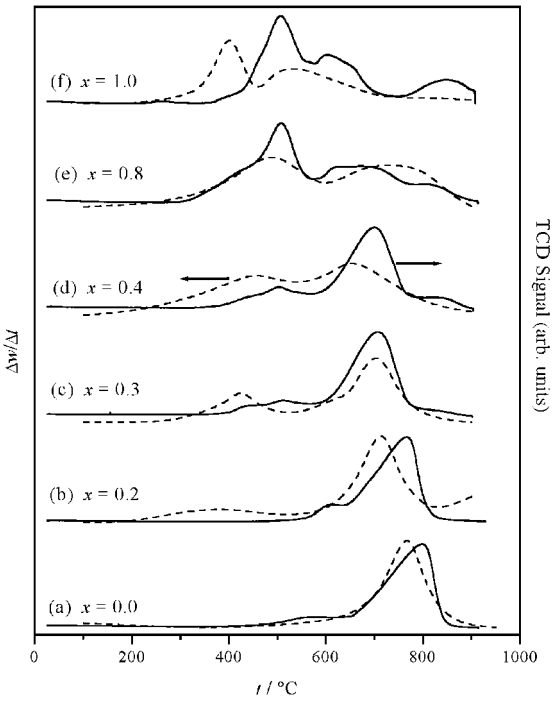

Fig. 2. TPR and DTG plots (dashed lines) of $LaMn_xV_{1-x}O_{4-\delta}$ samples as a function of x.

3.4. Dilatometry

The value of the percent linear thermal expansion of $LaVO_4$ and $LaMn_{0.5}V_{0.5}O_{4-\delta}$ samples, as obtained by dilatometric measurements, is plotted in Fig. 3 as a function of temperature. It was observed that while all the samples expand non-linearly with an increased rate of expansion up to 650 °C, the expansion beyond this temperature is quite different for the parent compound and the Mn-substituted samples. Thus, it is of interest to note that a negative thermal expansion is observed for $LaVO_4$ in the temperature range of

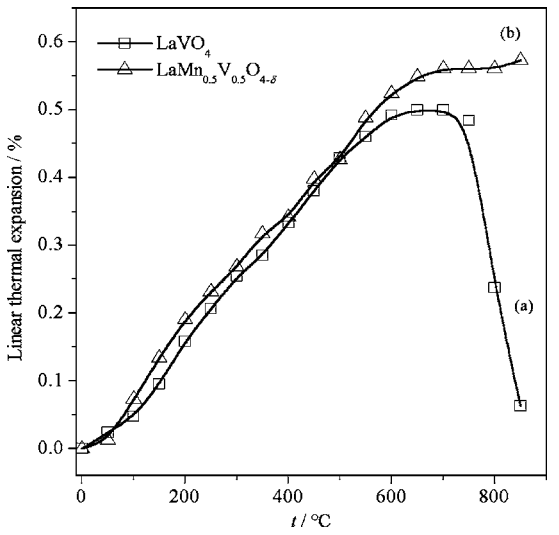

Fig. 3. Variation of % linear thermal expansion of $LaVO_4$ and $LaMn_{0.5}V_{0.5}O_{4-\delta}$ as a function of temperature.

Table 2
Thermal expansion behaviour of $LaVO_4$ and $LaMn_{0.5}V_{0.5}O_{4-\delta}$

Compound	Average linear thermal expansion coefficient ($\alpha_1 \times 10^6\ K^{-1}$)	
	25–650 °C	25–850 °C
$LaVO_4$	8.00	0.77
$LaMn_{0.5}V_{0.5}O_{3.7}$	8.78	6.95

650–800 °C. On the other hand the expansion in the case of $LaMn_{0.5}V_{0.5}O_{4-\delta}$ continues even at these high temperatures, though at lower rate. The values of average linear thermal expansion coefficient (α_l) of these samples are given in Table 2 for the temperature range of 30–650 °C and also for the entire temperature range of 30–800 °C. The drastic decrease in the value of α_l at elevated temperatures in case of $LaVO_4$ (Table 2) may be attributed to either contraction in cell volume or significant sintering of the sample at temperatures above 650 °C. Dilatometric measurements thus point to a better thermal stability of Mn-substituted samples as compared to that of the parent compound $LaVO_4$.

3.5. High-temperature X-ray diffraction

In order to explore the genesis of the thermal expansion behaviour of $LaVO_4$ at temperatures above 650 °C (Fig. 3a), the change of cell parameters and phase transitions effected by the thermal treatment were monitored by recording the HTXRD patterns at different temperatures up to 950 °C; these data are given in Fig. 4. It can be clearly seen that the $LaVO_4$ retained its single phase on heating at temperatures

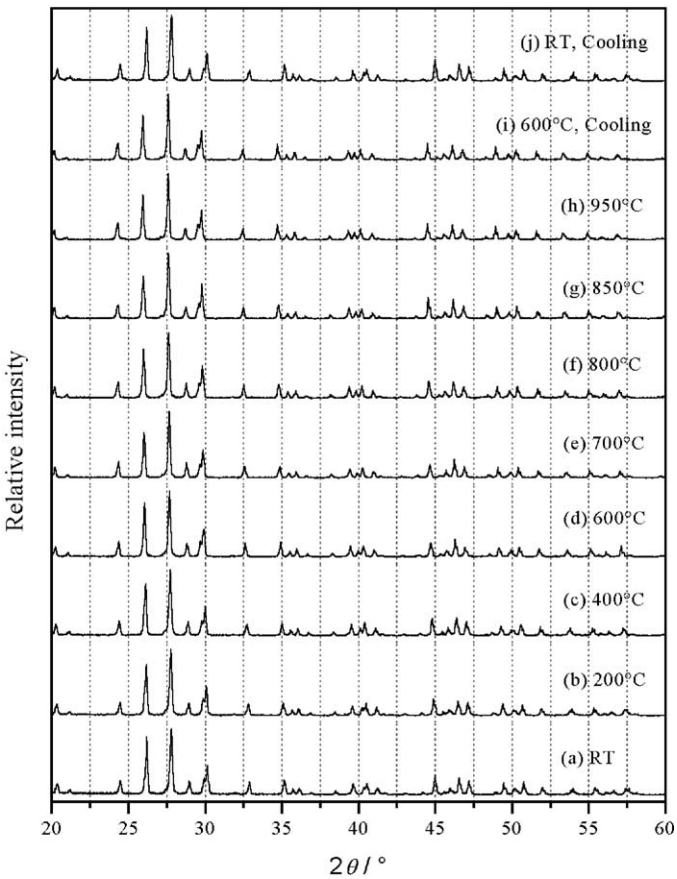

Fig. 4. HTXRD patterns of $LaVO_4$, recorded at different temperatures in the range of 28–950 °C and on subsequent cooling.

Table 3
Variation of unit cell parameters of $LaVO_4$ with temperature

Temperature (°C)	a (Å)	b (Å)	c (Å)	Volume (Å^3)
28	7.0530	7.2825	6.7047	333.15
200	7.0534	7.2881	6.7266	334.24
400	7.0684	7.2940	6.7481	336.10
600	7.0780	7.3052	6.7714	338.31
700	7.0907	7.3006	6.7813	339.18
800	7.0980	7.3108	6.7938	340.60
850	7.1004	7.3146	6.7978	341.08
950	7.1096	7.3196	6.8103	342.38

up to 950 °C though a systematic but marginal shift of 2θ-values towards a lower angle was observed with increasing temperature, e.g. the peak at 2θ-value of 30.11° shifts to 29.91° at 600 °C and to 29.75° at 950 °C. The cell parameters and the cell volumes of $LaVO_4$, as deduced from indexing of the XRD patterns in Fig. 4, are compiled in Table 3. The consistent increase in cell parameters and cell volume with increase of temperature unequivocally rules out the possibility of lattice contraction, as expected for these materials. Thus the drastic decrease in α_l at temperatures above 650 °C (Fig. 3a) is unquestionably attributed to the prevalence of sintering process in $LaVO_4$ at temperatures higher than 650 °C.

The effect of heating on lattice parameters, as shown in Table 3, was found to be reversible. Thus, on cooling of a sample subsequent to HTXRD data of Fig. 4h, the XRD patterns recorded at 600 °C (Fig. 4i) and at room temperature (Fig. 4j) were found to be identical with the corresponding patterns in Fig. 4d and a, respectively.

HTXRD patterns of $LaMn_{0.5}V_{0.5}O_{4-\delta}$ showed thermal expansion behaviour similar to that of La VO_4 at sample temperatures up to 850 °C. At higher temperatures, even though the peak position remained the same, the relative intensities of various lines were found to change marginally and in addition a partial loss of crystallinity was noticed in case of the samples with higher values of x. Using a technique of temperature-programmed desorption, we have demonstrated earlier that the substitution of V by Mn resulted in generation of non-stoichiometry in host $LaVO_4$, the extent of which increased with the manganese content [5]. It is well documented that the high aliovalent substitutions in ionic solids lead to the introduction of defect clusters in a lattice, which may have various configurations and may in turn hinder the mobility of the cations [7]. This mechanism may thus account for the resistance to sintering in case of the substituted $LaVO_4$ at elevated temperatures (Fig. 3).

4. Conclusions

Dilatometry and HTXRD techniques have been employed in this study in conjunction with TG and TPR methods so as to unravel the influence of B-site substitution in $LaVO_4$ on its thermo-physical characteristics. These results reveal that the substitution of V by Mn resulted not only in the lowering of the reduction temperature but also led to the resistance of host matrix to sintering at elevated temperature. Whereas the reduction of the substituted compositions occurred in two steps, $LaVO_4$ reduced to oxidation state V^{3+} in a single step. The presence of Mn^{4+} also assisted in the lowering of the temperature required for $V^{5+} \rightarrow V^{3+}$ transformation, probably due to oxygen ion vacancies generated in the VO_4^{3-} tetrahedra. The resistance to sintering of $LaMn_xV_{1-x}O_{4-\delta}$ compositions is attributed to introduction of certain defect clusters because of large non-stoichiometry in the anionic sublattice, which in turn might hinder the diffusion of the cations at elevated temperatures. It is suggested that the higher catalytic activity of the substituted samples and their reproducible reduction/re-oxidation behaviour during the repeated runs, as described in our earlier publication in detail [5], may have their origin in the lowering of the reduction temperature and the improved resistance to sintering as a result of the cationic substitution.

Acknowledgements

Authors thank Dr. A.K. Tyagi, Head, Solid State Chemistry Section, for the helpful discussions.

References

[1] B. Viswanathan, Catal. Rev.-Sci. Eng. 34 (1992) 337.
[2] C.S. Swamy, J. Christopher, Catal. Rev.-Sci. Eng. 34 (1992) 409.

[3] L.G. Tejuca, J.L.G. Fierro (Eds.), Properties and Applications of Perovskite-type Oxides, Marcel Dekker, New York, 1993.
[4] M.R. Pai, B.N. Wani, N.M. Gupta, J. Mater. Sci. Lett. 21 (2002) 1187.
[5] S. Varma, B.N. Wani, N.M. Gupta, Appl. Catal. A 205 (2001) 295.
[6] E. Wu, POWD Program, South Australia.
[7] P. Hagenmuller, Inorganic Solid Fluorides, Academic Press, London, 1985, p. 451.